Available online at www.sciencedirect.com
SCIENCE DIRECT®
PERGAMON
International Journal of Impact Engineering 28 (2003) 601–625
INTERNATIONAL JOURNAL OF IMPACT ENGINEERING
www.elsevier.com/locate/ijimpeng

How the airplane wing cut through the exterior columns of the World Trade Center

T. Wierzbicki*, X. Teng

Department of Ocean Engineering, Impact & Crashworthiness Laboratory, Massachusetts Institute of Technology, Room 5-218 77 Massachusetts Avenue, Cambridge, MA 02139-4307, USA

Received 20 April 2002

Abstract

The problem of the airplane wing cutting through the exterior columns of the World Trade Center is treated analytically. The exterior columns are thin-walled box beam made of high strength steel. The complex structure of the airplane is lumped into another box, but it has been found that the equivalent thickness of the box is an order of magnitude larger than the column thickness. The problem can be then modeled as an impact of a rigid mass traveling with the velocity of 240 m/s into a hollow box-like vertical member. The deformation and failure process is very local and is broken into three phases: shearing of the impacting flange; tearing of side webs; and tensile fracture of the rear flange. Using the exact dynamic solution in the membrane deformation mode, the critical impact velocity to fracture the impacted flange was calculated to be 155 m/s for both flat and round impacting mass. Therefore, the wing would easily cut through the outer column. It was also found that the energy absorbed by plastic deformation and fracture of the ill-fated column is only 6.7% of the initial kinetic energy of the wing.

Keywords: Aircraft impact; World trade center; Exterior column; Fracture

1. Introduction

The September 11th attack demonstrated the vulnerability of tall steel buildings to the impact of a fast moving airplane. Millions of terrified spectators around the world watched as the Boeing 767 moving with a cruising speed of 240 m/s (500 mph) hit the exterior wall of the World Trade Center (WTC), cut through it, and disappeared in the smoky cavity, Fig. 1, Ref. [1]. To the casual observer, it would appear that the facade of the Twin Towers did not offer any resistance at all,

*Corresponding author. Tel.: +1-617-253-2104; fax: +1-617-253-1962.
E-mail address: wierz@mit.edu (T. Wierzbicki).

0734-743X/02/$ - see front matter
PII: S0734-743X(02)00106-9

Nomenclature

$2a$	average height of the wing beam
b	breadth of the exterior column
c	stress wave speed
c_b	velocity of the propagating bending hinge
c_∞	asymptotic value of stress wave speed
E_0	initial kinetic energy
E_{tear}	tearing work of the webs
ΔE	total dissipated kinetic energy
F	tearing force
h	thickness of the exterior column
h_{eq}	equivalent thickness of the wing beam
l_w	wing span of the aircraft
m	mass per unit length of the beam
M	weight of the aircraft
M_0	mass of the rigid projectile
n	material hardening exponent
N_0	fully plastic axial force
q	plastic foundation resistance per unit length
Q	shear force
R	radius of the cylindrical projectile
t	time
t_1	time when the waves begin to propagate ahead of the contact point
t_f	final tearing time
V_0	impact velocity
V_1	velocity immediately after the impact on the front flange
V_2	velocity after cutting the web
V_3	velocity after cutting the rear flange
V_2^*	velocity after the impact on the web
$(V_0)_{cr}$	critical velocity to fracture the beam
w	transverse deflection
w'	slope
$\dot{w}$	transverse velocity
$\ddot{w}$	transverse acceleration
x	distance from the impact point

Greek symbols

α	wrapping angle of the cylindrical projectile
α_f	critical wrapping angle to fracture the beam
β	mass ratio in the case of the propagating hinge
ε	strain in the beam-string
ε_f	fracture strain

θ	propagation angle of the diverging crack
μ	mass ratio
ξ	wave front location
ρ	mass density
σ_0	plastic flow stress
σ_y	yield stress
σ_u	stress corresponding to the fracture strain

Fig. 1. A "clean" cut driven by the wings of a Boeing 767 into the facade of the North Tower.

and that the plane's wings and fuselage sliced through the exterior columns as if they were made of cardboard. This casual observation is confirmed by comparing the shape of the hole driven into the exterior walls with the outline of the plane. One can clearly see the position of the fuselage, two engines, and above all two symmetric narrow slots cut by the wings. A slightly larger opening was caused by the falling floor, which dragged the sections of the exterior columns inside the building. How was it possible that the relatively weak, light and airy airframe damaged the apparently heavy lattice of high strength steel columns? The devastating result of this encounter came as a surprise to the engineering and scientific community or at least to the present authors.

The objective of this research is not only to unravel the mystery behind this interactive failure but even more importantly to develop a general two-dimensional dynamic model of ductile fracture and break up of two beam-like structures of comparable strength hitting each other with high velocity. Such an undertaking will also be helpful in explaining subsequent stages of the impacts in which fragments of the airframe plowed through the truss-like floor of the WTC Towers and hit the core structure.

The airplane wing is a complex structure composed of open section beams, ribs, and skin reinforced by stringers. Upon impact by smaller objects such as hail, birds, etc. the leading edge of the airfoil will clearly be dented and the degree of damage will depend on the size and speed of the aircraft. The process of interactive failure of two deformable and fracturing bodies is very complex and could only be solved by means of numerical methods.

However, it was observed that if all structural members of the wing are lumped together and smeared into a box beam of equivalent mass, its thickness becomes over 100 mm which is ten times larger than the 9.5 mm thickness of the hollow external column of the Twin Towers. Therefore, in the first approximation, the impacting segment of the wing is treated as a rigid mass. The failure process of the exterior column is divided into three phases: instantaneous cutting through the front flange; tearing of side webs; and finally, tensile fracture of the rear flange. The impact problem is dominated by the local inertia of the box column so that plastic deformation and fracture are restricted to the immediate vicinity of the stricken part of the column. Each stage of the failure process is analyzed in the paper using the rigorous calculation method while still retaining the simplicity of the closed-form solutions.

It is recognized that the fuel in the wing tanks will greatly increase the mass per unit length of the wings and add to their devastating power. High velocity impact of fuel-filled tanks into deformable structures constitutes a challenging problem by itself and will be addressed in future research.

To the best of the author's knowledge, the problem of a thin-walled box beam subjected to high velocity impact of a rigid mass was not considered in the open literature. However, there are numerous theoretical and experimental studies dealing with projectile impact on thin plates. For a comprehensive review of the mechanics and physics of projectile impact, the reader is referred to the articles by Corbett et al. [2] and Goldsmith [3]. Hoo Fatt and Wierzbicki [4] showed that for relatively thin plates, where response is dominated by the membrane action, the critical impact velocity for penetration calculated on the basis of tensile necking or shear plugging was similar. Jones et al. [5] demonstrated through a thorough theoretical analysis that the energy absorbed by plastic deformation is dominated by the membrane response for thin plates (relative to the projectile radius). The contribution of shear increases with the plate thickness for lighter projectiles. This result was independently confirmed by Hoo Fatt et al. [6].

A comprehensive study on plastic response and fracture of beams loaded by a falling mass was undertaken by Jones and his co-workers [7–11]. They showed that thin beams fail by a combination of tensile necking and through thickness plugging. Based on extensive testing, a stress-based failure condition was established involving shear and membrane forces and bending moments [12]. Since most of the tests were performed in a drop tower facility with relatively large masses and slow impact speeds, the obtained results apply to a lower end of impact velocity spectrum up to 20 m/s.

Hoo Fatt and Wierzbicki [13] developed a theory of high velocity impact into free–free plastic beams and a beam supported by a plastic foundation. An interesting feature of this approach was a dual formulation that led to identical results. First, a local dynamic approach was taken leading to the wave equation with suitable boundary and initial conditions. Then, the same problem was formulated and solved using the principle of conservation of linear momentum. In both cases a characteristic velocity of propagation of lateral disturbances was identified which can serve as a convenient reference value for quantification of impact velocities. The above theory can also

predict the onset of fracture with relatively simple calculations. This theory was found to be particularly well suited for solving a difficult problem of a mass impact into a box beam that involves a complex interactive failure pattern. A similar problem was solved in a very rigorous way in Ref. [14] using a plastic wave propagation theory.

2. Structural modeling of the airplane

2.1. Wings

The operation weight of the Boeing 767 is taken to be $M = 120$ tons [1]. It is further assumed that the engine and wings contribute 25% each of the aircraft mass. Wings of modern transport aircraft are quite complicated structures consisting of open section beams, ribs, and a skin reinforced by stringers. Together they form a very stiff and strong box-type section. Determination of the strength of the wing relative to the strength of the building structure will require a detailed finite element analysis that we believe has not been performed to date. In order to retain the needed degree of simplicity, a computational model is developed in which the wing material is lumped into a single box-type beam. Assuming that this mass is now uniformly distributed over the whole length of the wing span l_w and that the beam is of a thin-walled square cross-section ($2a \times 2a$) with the thickness h_{eq}, the equivalent thickness of the wing beam is found from the equation

$$8ah_{eq}l_w\rho = \tfrac{1}{4}M, \tag{1}$$

where the left-hand side represents the mass of the box column and the right-hand side is the actual mass of the wings. Assuming an average height of the spar $2a = 0.48$ m and the span of the aircraft wing $l_w = 47.57$ m, the equivalent thickness becomes $h_{eq} = 122$ mm. The wings are swept at approximately 20° so that upon impact, external columns are contacted sequentially, one by one.

2.2. Exterior columns

The 64 m (208 ft) wide facade of the WTC Towers is, in effect, a prefabricated steel lattice. The exterior columns are narrowly spaced and finished with a silver-colored aluminum cladding. The main building block of the outer structure was a prefabricated element that was comprised of 3 floors, was 10.9 m high, and was 3.07 m wide, Fig. 2.

The prefabricated panel consisted of three columns connected by 3 transverse plates called spandrels. The breadth of the columns was $b = 356$ mm, and they were spaced 1000 mm apart from each other. The segments were staggered and bolted to their neighboring elements in every direction, Fig. 3. Each column was a box structure, almost square, with the wall thickness varying from 125 mm at the base of the building to 7.5 mm at the top. In the present analysis, we assume the wall thickness to be $h = 9.5$ mm [15]. There is some degree of uncertainty as to the grade of steel. We have assumed that the exterior columns were made of A36 high strength steel characterized by the yield stress $\sigma_y = 250$ MPa, ultimate strength $\sigma_u = 475$ MPa, hardening exponent $n = 0.2$, and uniaxial fracture strain $\varepsilon_f = 0.23$ [16]. The effect of stress triaxiality on

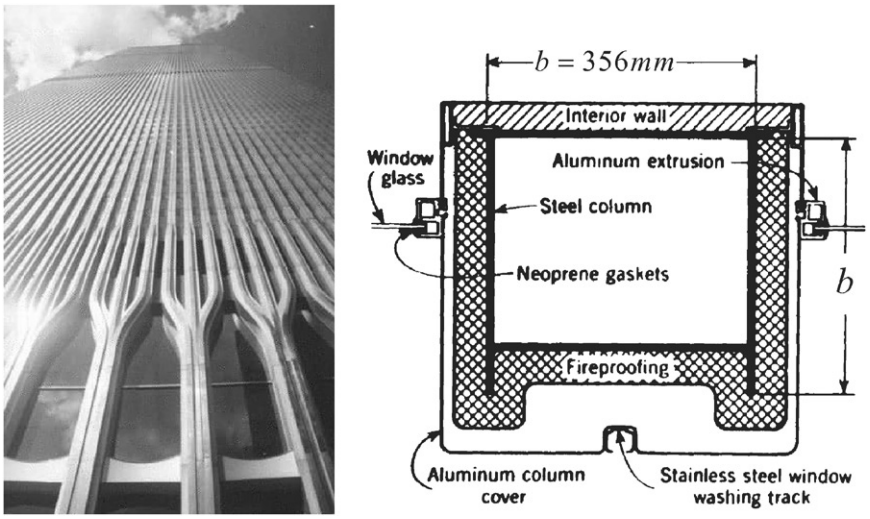

Fig. 2. Prefabricated lattice of external columns was made of welded high strength steel box sections.

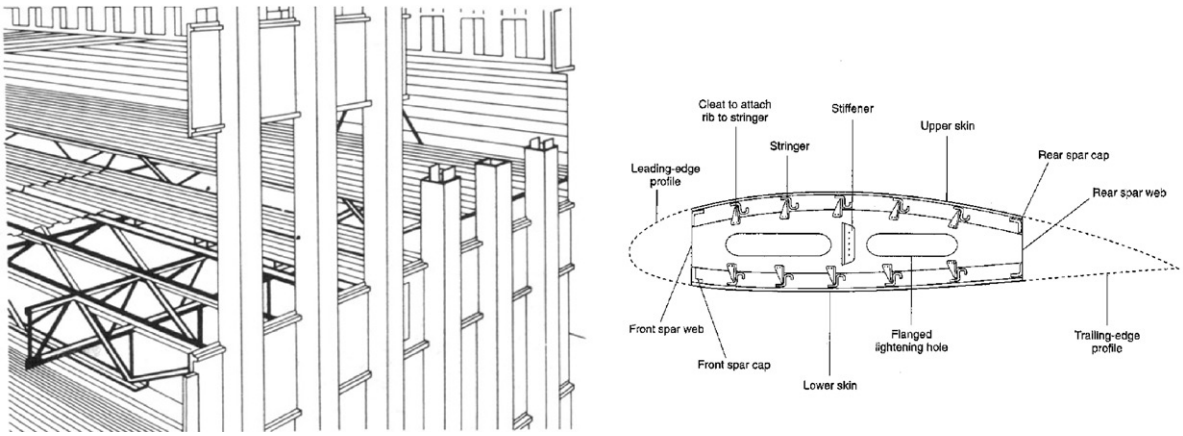

Fig. 3. Two opponents: the outer column and the wing. Note that the drawings are not in scale.

fracture is not considered because of lack of data. A more rigorous material fracture data will hopefully be available in the near future when test samples will be cut from the exterior columns to be retrieved from WTC Towers.

The so-called energy equivalent flow stress, calculated from the above values, and using the power-law approximation of the stress–strain curve, is $\sigma_0 = 396$ MPa. It was also pointed out in Ref. [15] that the yield stress of the exterior columns also varied in successive steps from 700 MPa at the bottom of the building to 295 MPa at the top.

In the first approximation, the airplane wings are modeled as a rectangular box beam. On comparing dimensions of the wing box with the dimension of the exterior columns, it is evident that the wall thickness of the former is an order of magnitude larger than the wall thickness of the

latter. Therefore, within the present level of accuracy, the wing can be considered a rigid body with a total mass M_0. This statement can be further reinforced by the observation that the fuel in the wing tanks could make the wings to behave more like rigid bodies. The mass of the portion of the wing that interacts with one column is obtained by dividing the total mass of the wings by the number of columns interacting with wings $M_0 = 30,000/50 = 600\,\text{kg}$. In reality, the failure process consists of multiple impacts of various structural elements of the wing into a stationary structure. A simple computational model of the multiple impact will be the subject of a separate publication [17].

3. Impact of a rigid mass into a box column

The deformation pattern of a box column hit by a rigid object moving with $V_0 = 240\,\text{m/s}$ is very localized due to the inertia and involves denting and stretching of the impacted flange and folding and tearing of the webs. The failure mode without and with fracture option was calculated by means of ABAQUS/explicit by Zheng and Wierzbicki [18], Fig. 4. At the critical velocity the fracture initiates. It will be calculated in subsequent sections. On increasing the impact velocity tensile and/or shear fracture will occur in the flange and will propagate down the web until full severance of the cross-section takes place. The details of this complex failure process are currently under investigation using numerical methods and the results are documented in Ref. [18]. For the purpose of the present analytical treatment, further simplifications are introduced. The box beam is broken into two flanges and two webs and a separate impact analysis is performed for each type of structure with the increasing level of complexity, Fig. 5.

First, the top flange is modeled as a long (or infinite) rigid-perfectly plastic beam/string that is supported by its own inertia. The length of the beam does not come into play because plastic deformations are localized around the impacted zone and we do not consider the entire range of impact velocities all the way to quasi-static loading. Clearly, for a statically loaded beam/string deformations would spread all the way to the support.

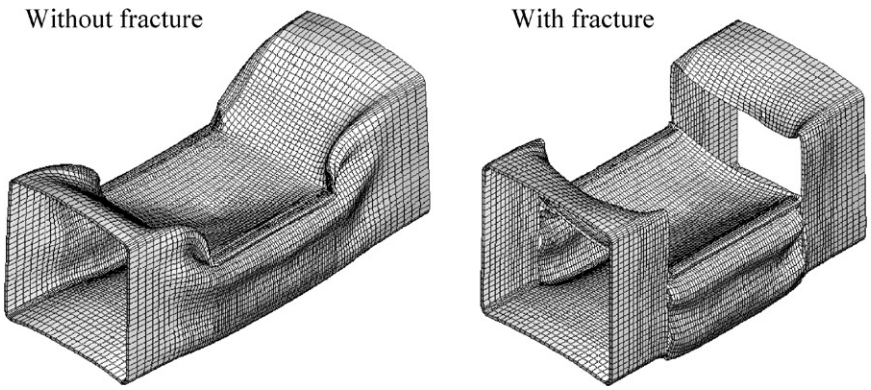

Fig. 4. Partially damaged box beam hit by a rigid cube at a speed of 240 m/s. Results of ABAQUS/explicit without fracture (left) and with fracture option (right).

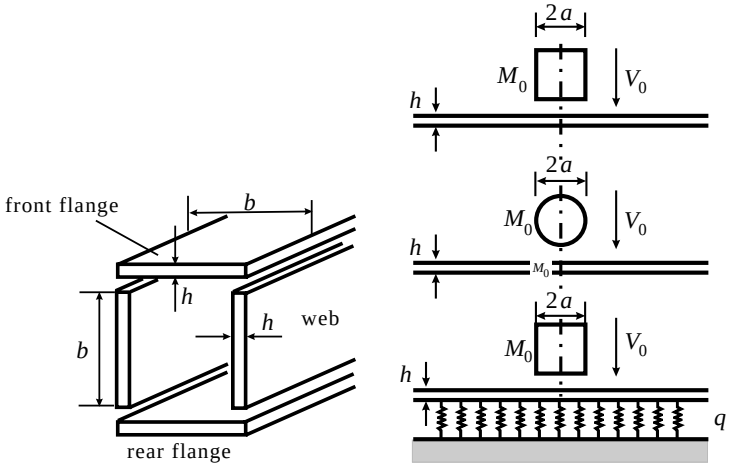

Fig. 5. Box beam broken into four components and three different models of the impact scenario.

The impacting mass is assumed to have a flat or circular leading edge. The latter case represents more realistically the actual shape of the wing. The most complex model involves plastic string resting on a rigid-plastic foundation. The foundation can be regarded as the resistance of the webs supporting the flange to the crushing load of the falling mass. In each of the three cases defined above, the analysis is first carried out without fracture. Then fracture is introduced and the critical impact velocity for the mass to perforate the beam/string is found. Finally, deformation and fracture of the rear flange are analyzed.

3.1. Blunt projectile impact into plastic string

Consider the top flange of the box beam and denote by h and b its thickness and width, respectively. The mass per unit length is $m = \rho hb$, where ρ is the mass density. The material of the flange is taken to be rigid-perfectly plastic defined by the flow stress σ_0. The flow stress is understood as the average value of the plastic stress over the strain path all the way to fracture:

$$\sigma_0 = \frac{1}{\varepsilon_f}\int_0^{\varepsilon_f} \sigma(\varepsilon)\,\mathrm{d}\varepsilon, \tag{2}$$

where ε_f is the plane strain fracture strain of a thin sheet. For a power-type stress–strain law with the exponent n, $\sigma = \sigma_u(\varepsilon/\varepsilon_f)^n$, the energy equivalent flow stress becomes $\sigma_0 = \sigma_u/(1+n)$, where σ_u is the stress corresponding to the fracture strain. The fully plastic axial force in the cross-section is defined by $N_0 = bh\sigma_0$.

From Fig. 4 one can infer that plastic deformation can be much larger than the plate thickness. Thus, the theory of moderately large deflections is appropriate with the dominant membrane action and insignificant bending resistance. But fracture of beams under high velocity impact may initiate quite early in the process when deflections are not large enough. Can the bending response also be neglected in this case? The answer to this legitimate question is obtained by comparing the propagation speed of flexural disturbances in a pure bending and pure membrane theory of beams. The "wave" speed in the bending theory is understood as a speed of propagating plastic

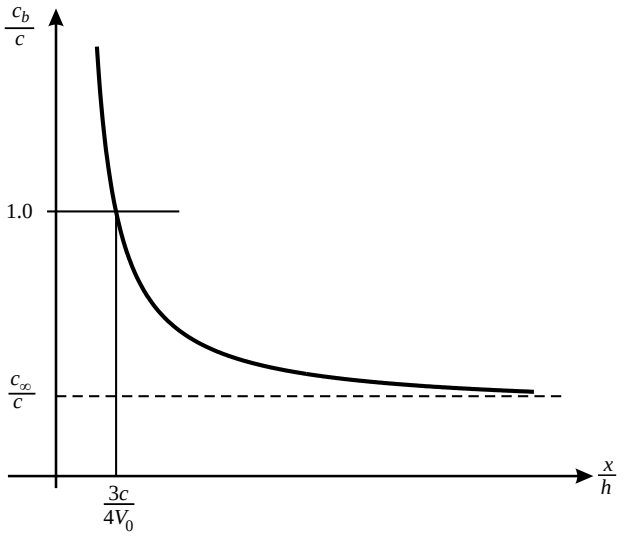

Fig. 6. Comparison of the wave speed of bending disturbance c_b with the speed of the membrane wave c.

hinge that carries information on the sudden mass impact. The solution to this problem has been worked out by Parkes [19] on an example of a cantilever beam impacted by the mass M_0 with the velocity V_0. The normalized velocity of the propagating hinge c_b is expressed by

$$\frac{c_b}{c} = \frac{3}{2}\frac{h}{x}\frac{c\,(1+(x/h)\,\beta)^2}{V_0\,(2+(x/h)\,\beta)}, \tag{3}$$

where x is the distance from the impacted end to the hinge, $\beta = mh/M_0$ is the mass ratio, and c is the reference speed $c = \sqrt{\sigma_0/\rho}$. For large distances x/h, the bending wave speed reaches a constant asymptotic value

$$\frac{c_\infty}{c} = \frac{3}{2}\left(\frac{hm}{M_0}\right)\frac{c}{V_0}. \tag{4}$$

At the same time, for small x/h, in the vicinity of the impacting site, Eq. (3) yields

$$\frac{c_b}{c} = \frac{3}{4}\frac{h}{x}\frac{c}{V_0}. \tag{5}$$

The bending wave speed is a rapidly diminishing function of the x-coordinate, Fig. 6. Additionally, c_b depends on the velocity and mass of the impacted body. This study is concerned with the range of impact velocities $V_0 \approx c$. It transpires from Eq. (5) that the wave speed of plastic hinge c_b is always smaller than the reference velocity c except for very short distances, less than the beam thickness. The above conclusion is not generally valid because the speed of the bending wave is not a constant for a beam but depends on the initial-boundary value problem. From the above analysis one can conclude that in the present high velocity impact the bending phase is insignificant.

The equation of motion of the plastic string undergoing moderately large deflection is [13,14]

$$(N_0 w')' = m\ddot{w}, \tag{6}$$

where $w(x,t)$ is the transverse deflection and primes and dots denote, respectively, differentiation with respect to the spatial coordinate x and time t. Therefore, use of the theory of moderately large deflection is appropriate here. Using the definition of N_0 and m introduced earlier, Eq. (6) takes the form of the wave equation

$$c^2 w'' = \ddot{w}, \tag{7}$$

where $c = \sqrt{\sigma_0/\rho}$ is the velocity of propagation of transverse plastic wave in the beam taken as reference velocity in Eq. (3). Depending on the magnitude of the flow stress and mass density, the wave speed is in the range of $c_{A36} = 224\,\mathrm{m/}$ for the A36 steel used in the WTC buildings with $\sigma_u = 475\,\mathrm{MPa}$ and $n = 0.2$. A similar value for an airplane aluminum structure with $\sigma_0 = 350\,\mathrm{MPa}$ and $\rho_{Al} = 2.7\,\mathrm{g/cm^3}$ is $c_{Al} = 360\,\mathrm{m/s}$. It should be noted that the aircraft impacted the South Tower at the speed of $V_0 = 240\,\mathrm{m/s}$ which is comparable to the wave speed. The present theory is applicable to the impact velocity of the order of c. Under these assumptions, the membrane wave c is always faster than the bending wave c_b, which proves general applicability of the present membrane theory. An order of magnitude higher or lower velocities would generate different failure modes and must be studied using different methods.

The equation of motion (7) is subjected to the following boundary conditions at the boundaries $x = a$ and $x = \xi = a + ct$:

$$(Q - N_0 w')\delta\dot{w} = 0, \tag{8}$$

where $2a$ is the width of the flat nose mass and Q is the shear force which is equilibrated by the vertical component of the membrane tension. At the impacted end $x = a$, each half of the beam is decelerating the rigid mass so that

$$N_0 w' = \tfrac{1}{2} M_0(1+\mu)\ddot{w} \quad \text{at} \quad x = a, \tag{9}$$

$$w = 0 \ \text{ at } \ x = \xi = a + ct, \tag{10}$$

where

$$\mu = \frac{2am}{M_0}. \tag{11}$$

The impact problem is subjected to the initial condition at $t = 0$

$$w = 0 \quad \text{for all } x, \tag{12}$$

$$\dot{w} = \begin{cases} V_1, & |x| \leqslant a, \\ 0, & |x| > a, \end{cases} \tag{13}$$

where the new initial velocity, V_1, is determined from the balance of linear momentum, as explained below.

At the instant of impact there is an instantaneous momentum transfer from the impacting mass M_0 moving with velocity V_0 to the new mass $M_0 + 2am$ moving with velocity V_1. Thus

$$V_1 = \frac{M_0}{M_0 + 2am} V_0. \tag{14}$$

In the case of the Twin Towers $M_0 = 600\,\mathrm{kg}$, $2a = 480\,\mathrm{mm}$, $b = 356\,\mathrm{mm}$, and $h = 9.5\,\mathrm{mm}$ so that $V_1 = 0.98 V_0 = 235.3\,\mathrm{m/s}$. The drop in the velocity is small. However, in the analysis of multiple

impact of smaller projectile into beams with comparable masses, Eq. (14) introduces a significant correction.

The solution to the initial-boundary value problem stated above follows the general procedure established in Refs. [4,13]. The discontinuity of the initial velocity generates shock waves that move at the speed c. All plastic deformations are concentrated at the wave front where material elements suddenly acquire transverse velocity $\dot{w}(t)$. In order to satisfy dynamic continuity

$$N_0 w'] + mc\dot{w}] = 0 \quad \text{at } x = \xi, \tag{15}$$

the deflection slope also suffers a jump at the wave front. Behind the wave front there is only a rigid body motion with the velocity diminishing in time. Because in the region behind the wave front $\ddot{w}$ and $\dot{w}$ are independent of the spatial coordinate x, Eq. (6) can be integrated with respect to x from $a<x<\xi$ to give

$$N_0 w'\big|_a^{\xi} - m(\xi - a)\ddot{w} = 0. \tag{16}$$

Using the boundary condition, Eq. (9), and the dynamic continuity condition, Eq. (15), the governing equation for the problem becomes

$$2cm\dot{w} + (M_0 + 2m\xi)\ddot{w} = 0 \tag{17}$$

subject to the initial condition. It is interesting to note that Eq. (17) can also be derived in a straightforward way from the conservation of linear momentum.

$$\frac{\mathrm{d}}{\mathrm{d}t}\{[M_0 + 2m\xi]\dot{w}\} = 0. \tag{18}$$

Thus, the local equilibrium approach and the global momentum conservation approach yield identical results provided the same uniform spatial distribution of the velocity profile is assumed. Integrating Eq. (17) once with respect to time and using the initial condition for velocities, Eq. (14), one gets

$$\dot{w} = \frac{V_1}{1 + \mu/(1+\mu)\, tc/a}. \tag{19}$$

A plot of spatial and temporal variation of the velocity field is shown in Fig. 7. The rate of the velocity drop depends strongly on the mass parameter μ.

The transverse displacement can be obtained by integrating the velocity field with respect to time

$$w(x,t) = \int_{t_1=(x-a)/c}^{t} \dot{w}(t)dt. \tag{20}$$

The presence of the non-zero lower limit in the above integral means that the beam acquires a displacement at point x only after the wave front arrives at that location at time $t_1 = (x-a)/c$. Substituting Eq. (19) into Eq. (20) and using Eq. (13), the transverse displacement becomes

$$w(x,t) = \frac{1+\mu}{\mu}\, a\, \frac{V_1}{c} \ln \frac{1 + \mu/(1+\mu)\, tc/a}{1 + \mu/(1+\mu)\, (x-a)/a}, \tag{21}$$

where the mass ratio μ is defined by Eq. (11).

The variation of the normalized deformed shape of the beam with time for two values of the mass ratio is depicted in Fig. 8. It can be seen that the slope is always maximum at $x = a$. The

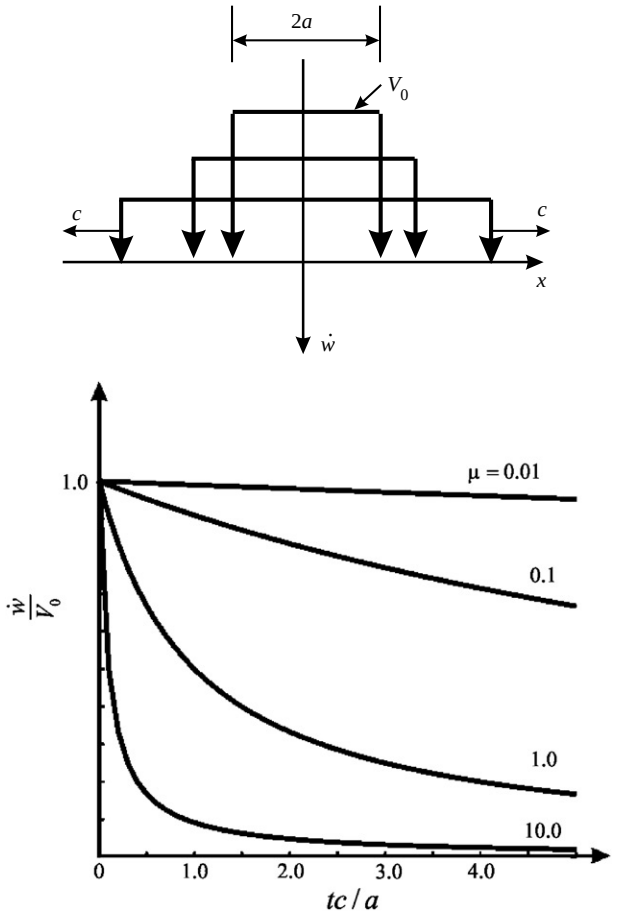

Fig. 7. Spatial and temporal variation of the transverse velocity of the flange.

maximum slope, obtained by differentiating Eq. (21) with respect to x, is

$$w'|_{x=a} = -\frac{V_1}{c} \tag{22}$$

and is independent of time. We are now in the position to predict the onset of fracture of the flange upon impact loading. The membrane strain in the axial direction is defined by

$$\varepsilon = \tfrac{1}{2}(w')^2. \tag{23}$$

It is assumed that fracture initiates when the maximum principal strain attains the plane strain necking strain in the flange ε_f, $\varepsilon_{max} = \varepsilon_f$. Combining Eqs. (22) and (23), the critical velocity to fracture becomes

$$(V_0)_{cr} = (1+\mu)c\sqrt{2\varepsilon_f} = (1+\mu)\sqrt{\frac{2\sigma_0\varepsilon_f}{\rho}}. \tag{24}$$

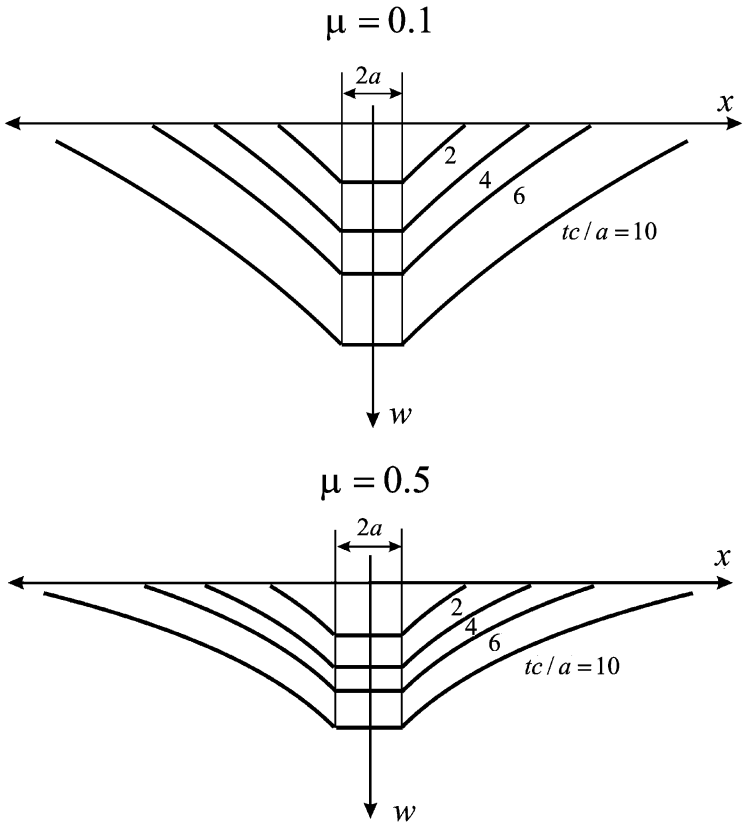

Fig. 8. Transient deflection profiles of the flange for the values of the mass ratio μ. Note a rigid body shift of the deformed portion.

It is seen that $(V_0)_{cr}$ depends on the mechanical properties of the material $(\sigma_0, \varepsilon_f, \rho)$ and the mass ratio. Taking for example $\varepsilon_f = 0.23$ for A36 steel as determined in Ref. [16], the critical impact speed to fracture the top flange of the exterior column is $(V_0)_{cr} = 0.69c_{A36} = 155\,\text{m/s}$. It can be concluded that the wing of the Boeing 767 traveling at $V_0 = 240\,\text{m/s}$ will immediately cut through the flange of the exterior column. It should be mentioned that the present method has previously led to a closed-form solution of the projectile impact into thin plates, [13], which correlated well with the experimental results due to Calder and Goldsmith [20].

3.2. Round projectile impact into plastic string

Let us assume that the impacting mass is a cylinder with the radius R. The transfer of momentum from the impacting mass to the flange occurs now over finite time as the string wraps around the circular shape projectiles. From Fig. 9 the axial coordinate of point A at which the mass loses contact with the flange and its velocity are given by

$$\xi = R\sin\alpha, \tag{25}$$

$$\dot{\xi} = \dot{\alpha}R\cos\alpha. \tag{26}$$

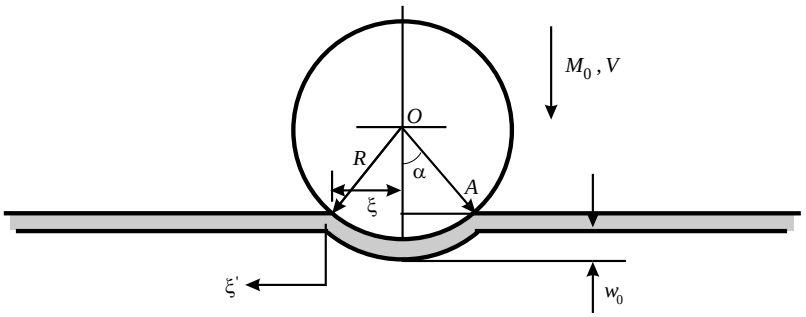

Fig. 9. Wrapping of the flange around the impacting cylinder in the initial supersonic phase of motion.

The vertical displacement and velocity are

$$w = R(1 - \cos\alpha), \tag{27}$$

$$\dot{w} = \dot{\alpha} R \sin\alpha. \tag{28}$$

Eliminating $\dot{\alpha}$ between Eqs. (26) and (28), the propagation velocity of contact point A is

$$\dot{\xi} = \frac{\dot{w}(t)}{\tan\alpha}. \tag{29}$$

Initially $\dot{w}(0) = V_0$ and $\alpha = 0$. Therefore, $\dot{\xi}(\alpha) \to \infty$ and point A travels at a "supersonic" velocity $\dot{\xi} > c$. This means that no information on the deformation can propagate ahead of the contact point and the flange must wrap up around the lateral surface of the cylinder. This phase lasts until the speed $\dot{\xi}$ becomes equal to c or fracture occurs first.

The time change of the downward velocity is obtained from the conservation of linear momentum

$$(M_0 + 2\xi m)\dot{w} = M_0 V_0, \tag{30}$$

$$\frac{\dot{w}(\alpha)}{V_0} = \frac{M_0}{M_0 + 2m\xi} = \frac{1}{1 + \mu\sin\alpha}. \tag{31}$$

The above solution is valid until the velocity $\dot{\xi}$ reaches a sonic value c which gives $\dot{w}(t) = c\tan\alpha$ or using Eq. (23) fracture takes place at $\alpha_f = \tan^{-1}\sqrt{2\varepsilon_f}$. Two typical situations may occur as illustrated in Fig. 10.

At a larger value of the parameter μ, the solution intersects the line $\dot{w} = c\tan\alpha \approx c\alpha$ before fracture occurs. The first phase of the motion terminates at $\alpha = \alpha_1$, defined by the solution of the following quadratic equation:

$$c\tan\alpha_1 = \frac{V_0}{1 + \mu\sin\alpha_1}. \tag{32}$$

If the beam does not break in the supersonic phase, the waves will propagate ahead of the contact point. In the subsonic phase, the transverse velocity can also be obtained from the

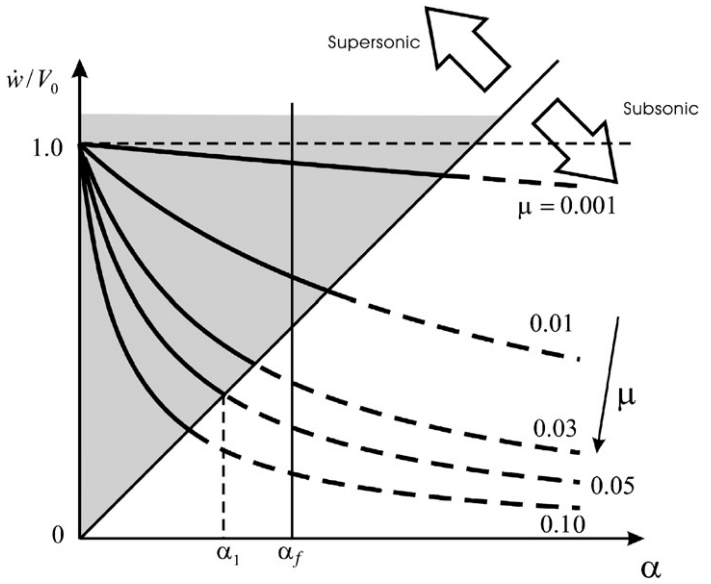

Fig. 10. Solution in the supersonic range is bounded by fracture angle α_f or by the boundary with the subsonic region, whichever occurs first.

momentum conservation by assuming the uniform distribution in space,

$$\frac{\dot{w}}{V_0} = \frac{M_0}{M_0 + 2mR\sin\alpha + 2mc(t-t_1)} = \frac{1}{1+\mu\sin\alpha + \mu c(t-t_1)/R}, \tag{33}$$

where the waves begin to propagate ahead of the contact point at $t = t_1 = R\sin\alpha_1/c$. The deflection of the beam ahead of the contact point is given by

$$w = \int_{(x-R\sin\alpha)/c+t_1}^{t} \dot{w}\,\mathrm{d}t. \tag{34}$$

Substituting the expression for the velocity, one obtains the deflection of the beam by integrating the above equation

$$\frac{w}{R} = \frac{1}{\mu}\frac{V_0}{c}\ln\frac{1+\mu\sin\alpha + \mu(c(t-t_1))/R}{1+\mu(x/R)}. \tag{35}$$

Instantaneous deflection profiles calculated from Eq. (35) are shown in Fig. 11.

By differentiating the deflection of the beam with respect to the spatial coordinate x, one arrives at the expression for the tensile strain

$$\varepsilon = \frac{1}{2}\left(\frac{V_0}{c}\right)^2\left(\frac{1}{1+\mu(x/R)}\right)^2, \quad \frac{x}{R} \geqslant \sin\alpha. \tag{36}$$

It can be observed from the above equation that tensile strain in the beam ahead of the contact point decreases with distance from the contact point. The tensile strain in the wrapped part

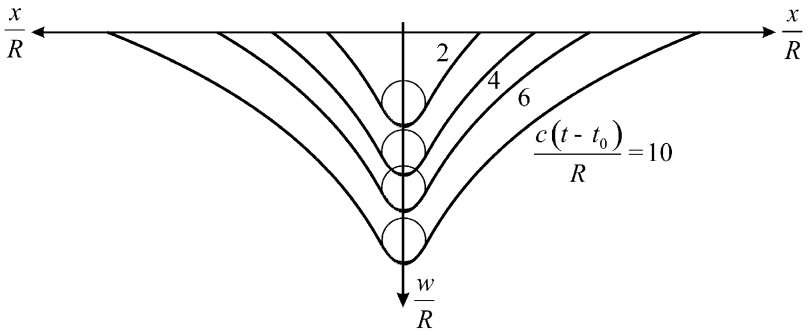

Fig. 11. Transient deflection profiles of the flange under impact of a circular projectile ($\mu = 0.5$).

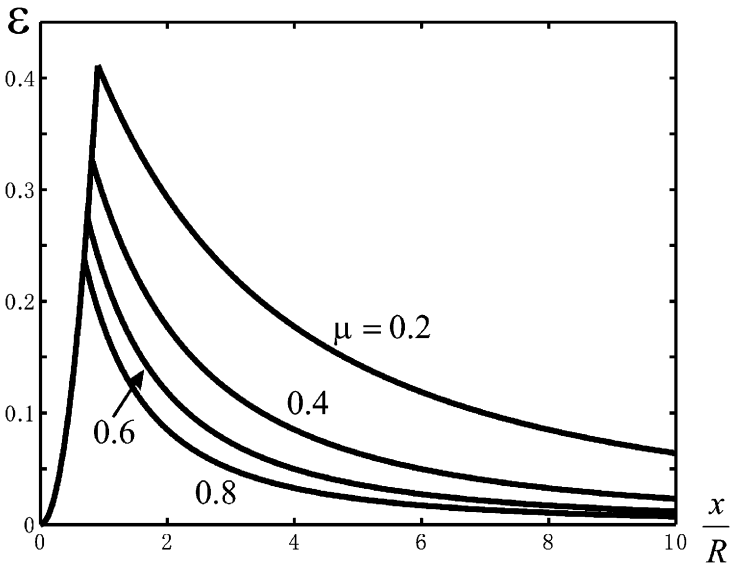

Fig. 12. Tensile strain versus spatial coordinate for different mass ratios.

around the circular projectile can be expressed as

$$\varepsilon = \frac{1}{2}\left(\frac{x}{R}\right)^2, \quad 0 \leqslant \frac{x}{R} \leqslant \sin\alpha. \tag{37}$$

Plots of the tensile strain variation along the beam for different mass ratios are show in Fig. 12. It can be seen that smaller mass ratios give larger tensile strain. Or say, it is more likely that the beam will fracture in the case of the projectiles with small impact masses and high impact velocity. Also, the maximum tensile strains always occur at the contact point. Hence, it can be concluded that if the beam does not break in the supersonic phase, it will not break at all.

Because the maximum tensile strains always occur at the contact point, the critical impact velocity can be defined by setting the tensile strain in the contact point equal to the fracture strain, that is, let α_1 in Eq. (32) be equal to α_f,

$$\frac{(V_0)_{cr}}{c} = \left(1 + \mu\sqrt{\frac{2\varepsilon_f}{1+2\varepsilon_f}}\right)\sqrt{2\varepsilon_f}. \tag{38}$$

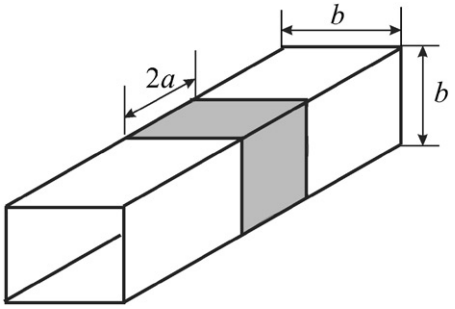

Fig. 13. Elements of the box beam participating in the initial momentum transfer (shaded area).

In summary, if the impact velocity is smaller than the critical velocity, the beam will never fracture, and the wave will propagate ahead of the contact point. If, on the other hand, the impact velocity is larger than the critical velocity, the beam will fracture in the supersonic phase. On comparing Eqs. (24) and (38), one can observe that the critical impact velocity in the case of the circular projectile is smaller than that of the blunt projectile.

For example, in the case of the wing impact to exterior column, the critical impact velocity to fracture the flange of the exterior is $(V_0)_{cr} = 0.68c_{A36} = 154\,\mathrm{m/s}$, which is only 1 m/s lower than that in the case of the blunt projectile. Hence, the same conclusion can be drawn that the wing of the Boeing 767 modeled as a rounded-off structure traveling at $V_0 = 240$ m/s will cut through the flange of the exterior column.

3.3. Response of a flange on foundation

We return now to the original box columns which is composed of the top flange, two webs and the bottom flange, Fig. 5. The problem is modeled as one with multiple impact. First the wings hit the top flange and the common velocity after impact is given by Eq. (14). Next, the new mass $(M_0 + 2ma)$ is colliding with two webs. Following Zhang and Yu [21], there will be an instantaneous momentum transfer between $(M_0 + 2ma)$ and the new total mass of $(M_0 + 6ma)$, Fig. 13. Thus, the velocity after the second impact is

$$V_2^* = \frac{M_0 + 2ma}{M_0 + 6ma} V_1. \tag{39}$$

Thus, after the second impact the velocity of the colliding mass, now traveling with the top flange and two webs, is

$$V_2^* = \frac{M_0}{M_0 + 6am} V_0 = \frac{1}{1 + 3\mu} V_0 = 0.94 V_0 = 225.6\,\mathrm{m/s}. \tag{40}$$

Tam and Calladine [22] developed a modified theory where the momentum transfer proceeds in a more gradual way. The case of a gradual momentum transfer is described next.

The question is to what extent the presence of the web modifies the onset of fracture of the flange. Right after the impact the two walls offer a full compressive resistance $q = 2h\sigma_0$ (per unit length). Later on the web plates will buckle plastically and fold developing a complex bi-axial stress state but we are interested in the initial response. As shown in Fig. 14, the box column

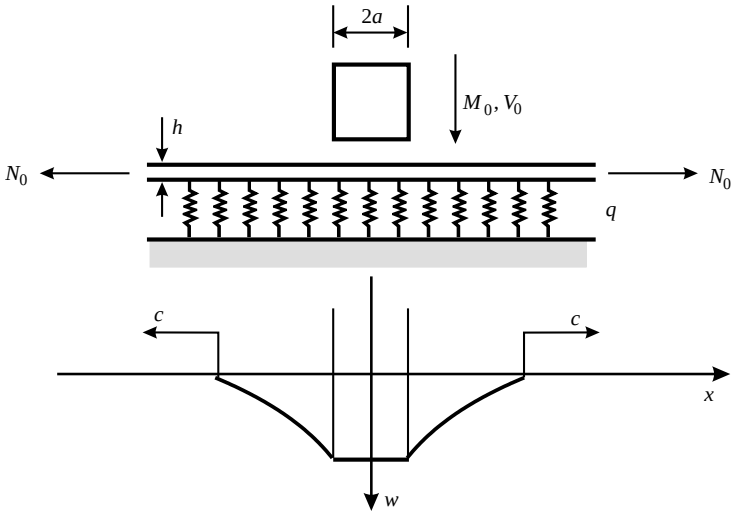

Fig. 14. Notation used in the string model on plastic foundation.

can now be modeled as a string on plastic foundation that is described by the inhomogeneous wave equation

$$c^2 w'' = \ddot{w} + \frac{2c^2}{b} \tag{41}$$

subject to the same boundary and initial condition.

The solution method to this problem was developed by Hoo Fatt and Wierzbicki [13]. In the present notation, the velocity function is given by

$$\dot{w}(t) = \frac{(1+\mu)V_1 - (2qa^2/M_0c)(tc/a) - (qa^2/M_0c)(tc/a)^2}{(1+\mu) + \mu(tc/a)}. \tag{42}$$

Integrating Eq. (38) in time, according to Eq. (20), one can get the expression for the displacement, slopes, and maximum slope. In particular, the maximum slope occurs as before at $x = a$ and is given by

$$(w')_{\max} = -\frac{V_1}{c} \tag{43}$$

that is independent of the foundation constant q. The independence of the maximum slope and thus fracture on the foundation constant is very significant because of the uncertainty in choosing the right value for the foundation constant.

3.4. Tearing of the webs

The instantaneous fracture of the flange initiates the process of tearing of the webs. The fracture process is assumed to follow the pattern of the so-called "concertina tearing" initially developed for quasi-static loading [23,24]. The process involves two diverging cracks emanating from the initial cut that runs at approximately $\theta = 14^\circ$ from the vertical direction, Fig. 15. The plate between the cracks folds back and forth with a relatively short wavelength. A limited numerical

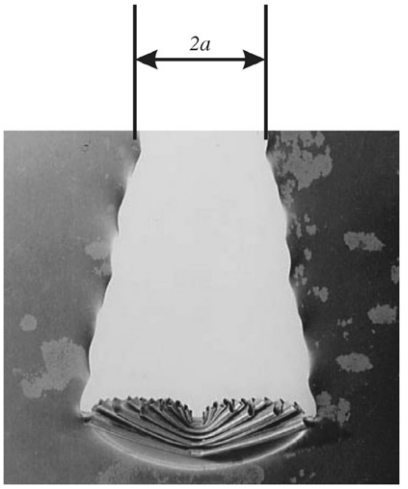

Fig. 15. Webs are assumed to fail in the concertina tearing mode with diverging cracks. Shown in the photo are the results for a much thinner plate. The WTC Tower columns will develop just fewer folds (see Fig. 4).

simulation performed by Zheng and Wierzbicki [18] confirms that this type of folding is observed under high velocity impact (see Fig. 4).

Therefore, it is reasonable to assume that the local lateral inertia of the folding webs will not alter the expression for the total resisting force. From Ref. [23] the force necessary to fold and tear one plate with two diverging cracks is

$$F = 3\sigma_0(2a)^{1/3}h^{5/3}, \tag{44}$$

which for the present numerical example yields the value $F = 0.396\,\mathrm{MN}$. Now considering that the momentum transfer occurs in a gradual way, the equation of motion is

$$2F = -\frac{\mathrm{d}}{\mathrm{d}t}\left[\left(M_0 + 2ma + 4ma\frac{w}{b}\right)\dot{w}\right] \tag{45}$$

with zero initial conditions for displacement and the initial velocity $V_1 = 0.98V_0$. The solution of the above equation is

$$\dot{w} = \frac{2Ft + (M_0 + 2ma)V_1}{M_0 + 2ma + 4ma(w/b)}. \tag{46}$$

The above differential equation can be integrated through the separation of variable and the displacement of the impacting mass in contact with the web is given by

$$2ma\frac{w^2}{b} + (M_0 + 2ma)w = Ft^2 + (M_0 + 2ma)V_1 t, \tag{47}$$

where the initial condition was used, $w = 0$ at $t = 0$. The above equation is also a quadratic equation with respect to time t. The final tearing time t_f can be determined by setting $w = b$ in Eq. (47):

$$t_\mathrm{f} = \frac{-(M_0 + 2ma)V_1 + \sqrt{[(M_0 + 2ma)V_1]^2 + 4F(M_0 + 4ma)b}}{2F}. \tag{48}$$

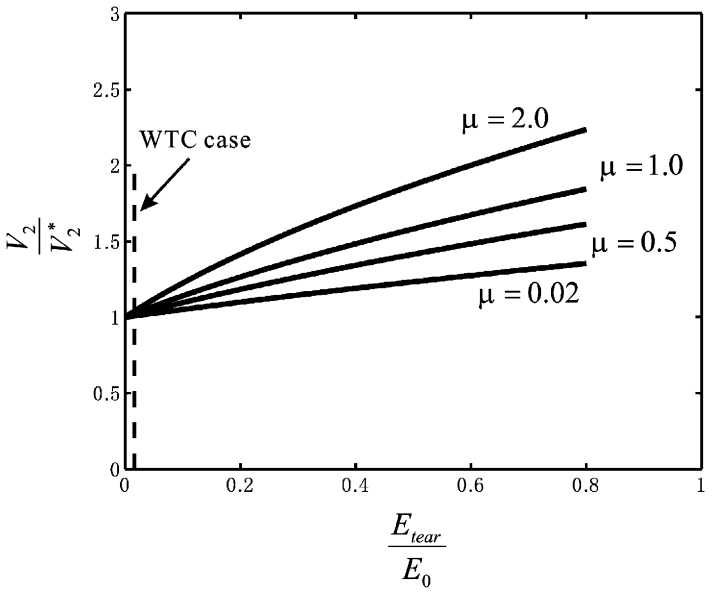

Fig. 16. Ratio of the velocity at the end of the tearing phase versus energy ratio for different mass ratios.

Substituting the expression for t_f and setting $w = b$ in Eq. (46), one arrives at the velocity V_2 at the end of the tearing phase

$$V_2 = \frac{\sqrt{[(M_0 + 2ma)V_1]^2 + 4F(M_0 + 4ma)b}}{M_0 + 6ma}. \tag{49}$$

Note that in the limiting case of zero shear force, $F = 0$, Eq. (49) reduces to the previous result which is based on the method of instantaneous momentum transfer, Eq. (39). The velocity ratio between the gradual moment transfer solution and the instantaneous moment transfer solution is given by

$$\frac{V_2}{V_2^*} = \sqrt{1 + \frac{2Fb}{\frac{1}{2}M_0V_0^2}(1 + 2\mu)} = \sqrt{1 + \frac{E_{\text{tear}}}{E_0}(1 + 2\mu)}, \tag{50}$$

where $E_{\text{tear}} = 2Fb$ is the tearing work of the webs; and $E_0 = \frac{1}{2}M_0V_0^2$ is the initial kinetic energy of the impacting mass. Plots of the ratio of V_2 to V_2^* versus the energy ratio of E_{tear} to E_0 for different mass ratios μ are given in Fig. 16.

For small values of the parameter, E_{tear}/E_0, Eq. (50) can be approximated by using Taylor series expansion:

$$\frac{V_2}{V_2^*} \approx 1 + \frac{1}{2}\frac{E_{\text{tear}}}{E_0}(1 + 2\mu). \tag{51}$$

Using the data of the particular example, the energy ratio is $E_{\text{tear}}/E_0 = 0.28/17.28 = 0.016$; and the mass ratio is $\mu = 0.02$; the velocity at the end of the tearing phase is $V_2 = 1.008\ V_2^* = 227.4\,\text{m/s}$, which is almost the same as the velocity obtained by the method of instantaneous momentum transfer. This indicates that the tearing resistance does not affect much the

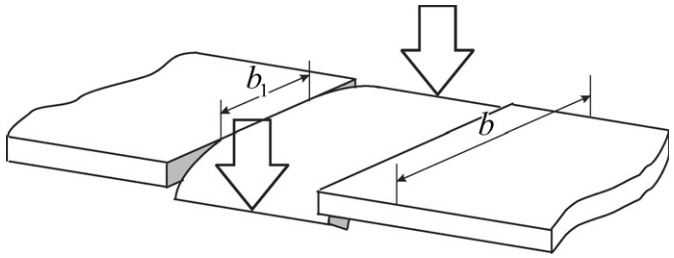

Fig. 17. Initial phase of failure of the rear flange with the out-of-plane (Mode III) fracture.

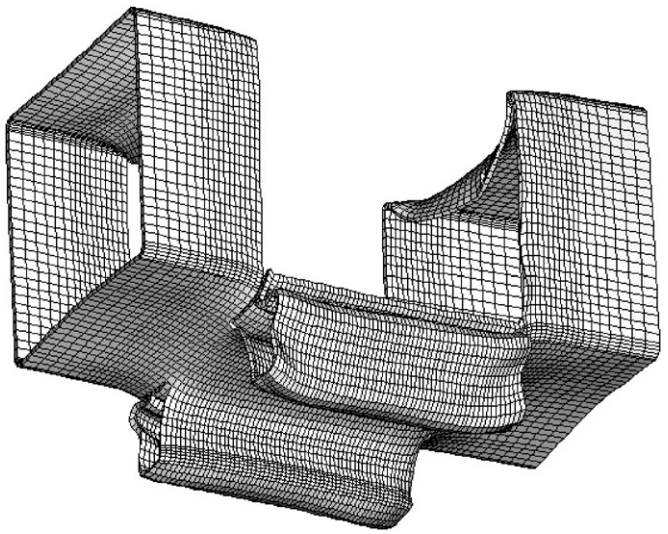

Fig. 18. Finite element simulation showing a combined Mode I/Mode III fracture pattern.

momentum transfer. However, it should be mentioned that in the case with large mass ratio, the difference between the velocity V_2 and V_2^* could be significant. With the velocity V_2 we are entering the final stage of the failure process which is fracture of the rear flange.

3.5. *Fracture of the rear flange*

Failure of the back flange is quite complex and involves at least two distinct phases. The crack in the diverging concertina mode turns at 90° after reaching the lower edge of the box column. After that the out-of-plane shearing cracks are formed and propagate some distance towards each other, Fig. 17. At the same time two segments of the back flange are subjected to a combined shear and tension and finally the remaining ligament necks and fractures on reaching the fracture strain. The above failure sequence was confirmed by a finite element solution of the exterior column, shown in Fig. 18 [18].

The failure mechanism of the rear flange is thus different from that of the top flange. For both the cases, the energy dissipated to break the flange is small compared to the energy lost during the momentum transfer (only 4.3%) [25]. Therefore, the momentum conservation alone can be used

to determine the final (exit) velocity of the impacting mass

$$V_3 = \frac{M_0 + 6ma}{M_0 + 8ma} V_2 = 223.2\,\mathrm{m/s} \tag{52}$$

It is not clear where the energy lost in the momentum transfer goes into. Clearly, there must be a complex system of incident and reflected plastic waves through the thickness accompanied by a plastic flow and change in the wall thickness.

3.6. Energy dissipation

The initial kinetic energy of the portion of the wing impacting one exterior column is

$$E_0 = \tfrac{1}{2} M_0 V_0^2 = 17.28\,\mathrm{MJ}. \tag{53}$$

(Note that this is only 0.5% of the total kinetic energy of the entire plane.) The energy dissipated in the failure of the impacted top flange, two webs and bottom flange can be calculated from the known drop of the mass velocity during the momentum transfer:

$$\Delta E_{\text{top flange}} = \tfrac{1}{2} M_0 V_0^2 - \tfrac{1}{2}(M_0 + 2ma) V_1^2 = 0.352\,\mathrm{MJ}, \tag{54}$$

$$\Delta E_{\text{web}} = \tfrac{1}{2}(M_0 + 2ma) V_1^2 - \tfrac{1}{2}(M_0 + 6ma) V_2^2 = 0.484\,\mathrm{MJ}, \tag{55}$$

$$\Delta E_{\text{bottom flange}} = \tfrac{1}{2}(M_0 + 6ma) V_2^2 - \tfrac{1}{2}(M_0 + 8ma) V_3^2 = 0.303\,\mathrm{MJ}. \tag{56}$$

Note that in the process of concertina tearing of the webs energy dissipated has been included in Eq. (55). The above fractional energies give a total loss of kinetic energy

$$\Delta E_{\text{total}} = \Delta E_{\text{top flange}} + \Delta E_{\text{web}} + \Delta E_{\text{bottom flange}} = 1.139\,\mathrm{MJ}, \tag{57}$$

which is illustrated in a graphical form in Fig. 19. This represents approximately 6.7% of the initial kinetic energy of the relevant portion of the wing. The present detailed analysis of the failure process confirmed in general terms previous estimates on the energy needed to cut through the exterior columns based on a simple plastic shear model [1]. Finally, the predicted wing velocity versus the travel time is shown in Fig. 20, and compared to the finite element results obtained in Ref. [18]. The correlation is good considering the simplicity of the closed-form solution.

The agreement of the present closed-form solution and ABAQUS calculation is perfect in the phase of cutting through the flange and web up to the time of 1.6 ms. The error in the third phase is explained by observing that the rear flange does not fracture instantaneously by shear but it is dragged for a long time and failed by a combination of the out-of-plane shear and tension. The initial impact velocity 240 m/s drops to the exit value of 223.2 m/s and this will be the entry velocity that will subsequently damage the floors and core structure of the Twin Towers.

The final conclusion of the present calculation is that the exterior column, despite its mighty appearance, dissipated only 6.7% of the initial kinetic energy of the relevant portion of the wing. This means that the remaining 93.3% of the energy was then used to damage the interior of the Twin Towers, i.e., floors and the core structure.

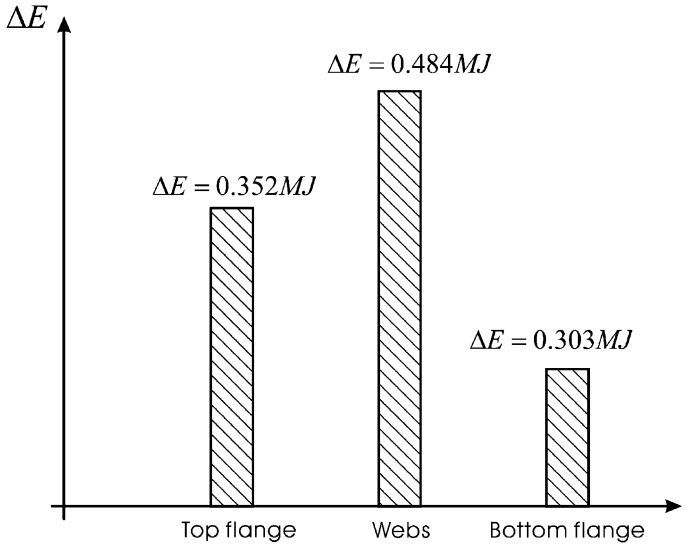

Fig. 19. Fractional energy loss for the top flange, two webs, and bottom flange, respectively.

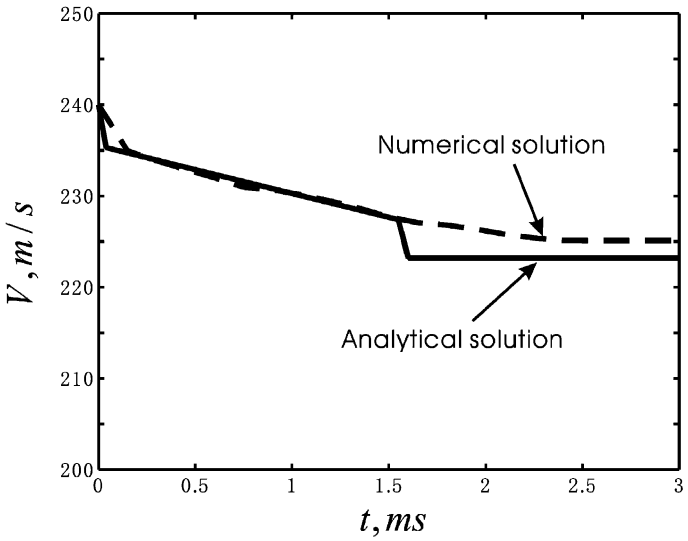

Fig. 20. Variation of the wing velocity as a function of the cutting time.

4. Conclusions

In this paper, we have analyzed the sequential failure of a typical exterior column of the World Trade Center Towers subjected to the impact of the airplane wing traveling at 240 m/s. It was found that the fracture process started immediately and continued as plate tearing on the side webs to be completed as tensile/shear fracture on the rear flange. In each stage, the resisting forces arising from plastic deformation and fracture were calculated and the time history of the velocity of the impacting wing section was determined.

The minimum impact velocity to cause fracture was determined from Eq. (24) to be 155 m/s. Should the aircraft be traveling not at a cruising speed but at a much lower take-off or landing speed of 200 mph (about 100 m/s), then the exterior columns would appear to have deflected the wings without fracture.

It is concluded that the process of wing cutting through the exterior columns dissipated only 1.139 MJ of energy. This constitutes only 6.7% of the initial kinetic energy of the wing. The remaining 93.3% of the kinetic energy was then transferred into the interior of the building causing fatal damage to the floors and core structure. The present analysis introduced a substantial correction to the earlier estimate of the energy required to shear the column reported in Ref. [1] but in each case the energy to break the airplane wing through the exterior facade of the Twin Towers is insignificant.

The present analysis also suggested that the exterior column would be able to stop the airplane wing or at least prevent a local shear failure if the average flow stress of the material is increased by a factor of two. Thus, had the plane hit the base of the Towers which were made of high strength steel with the yield stress of $\sigma_y = 700$ MPa, the airplane might have been deflected by the exterior walls.

All of the above conclusions must be treated as tentative because the actual wing was composed of several much thinner members and not one thick beam. Also the effect of the fluid inside the fuel tanks that are placed within the wing boxes is not considered. The analysis of a multiple impact of two hollow beams of a similar strength will be presented in a separate publication [17].

Acknowledgements

Thanks are due to Li Zheng for providing us with the results of the preliminary numerical calculations and to Liang Xue for his help in getting the relevant photographic material.

References

[1] Wierzbicki T, Xue L, Hendry-Brogan M. Aircraft impact damage of the world trade center towers. MIT Impact and Crashworthiness Laboratory, Technical Report 74, February 2002, also Towers lost and Beyond. TWI Press, September 2002.
[2] Corbett GG, Reid SD, Johnson W. Impact loading of plates and shells by free-flying projectiles: a review. Int J Impact Eng 1996;18(2):141–230.
[3] Goldsmith W. Non-ideal projectile impact on targets. Int J Impact Eng 1999;22(2-3):95–395.
[4] Wierzbicki T, Hoo Fatt MS. Deformation and perforation of a circular membrane due to rigid projectile impact. In: Geers TL, Shin YS, editors. Dynamic response of structures to high energy excitation, vol. 225. New York: ASME, 1997.
[5] Jones N, Kim SB, Li QM. Response and failure of ductile circular plates struck by a mass. J Press Vess-T Trans ASME 1997;119(3):332–42.
[6] Hoo Fatt MS, Liu Y, Wang ZB. Plastic deformations of impulsively loaded, rigid-plastic beams. J Eng Mech-ACSE 2000;126(2):157–65.
[7] Jones N. Plastic failure of ductile beams loaded dynamically. J Eng Ind Trans ASME Ser B 1976;98(1):131–6.
[8] Yu J, Jones N. Further experimental investigations on the failure of clamped beams under impact loads. Int J Solids Struct 1991;27(9):1113–37.

[9] Liu JH, Jones N. Dynamic response of a rigid plastic clamped beam struck by a mass at any point on the span. Int J Solids Struct 1988;24(3):251–70.
[10] Liu JH, Jones N. Experimental investigation of clamped beams struck transversely by a mass. Int J Impact Eng 1987;3:303–35.
[11] Jones N. Structural impact. Cambridge: Cambridge University Press, 1989.
[12] Jones N, Shen WQ. Criteria for inelastic rupture of metal beams subjected to large dynamic loads. In: Jones N, Wierzbicki T, editors. Structural crashworthiness and failure. Amsterdam: Elsevier, 1993.
[13] Wierzbicki T, Hoo Fatt MS. Impact response of a string-on-plastic foundation. Int J Impact Eng 1992;12(1):21–36.
[14] Mihailescu-Suliciu M, Sulicio I, Wierzbicki T, Hoo Fatt MS. Transient response of an impulsively loaded plastic string on a plastic foundation. Q Appl Math 1996;LIV(2):327–43.
[15] Hart F, Henn W, Sontag H. In: Godfrey GB, editor. Multi-story buildings in steel. Cambridge, UK: University Press, 1985.
[16] Muragishi O. Premature Cleavage of Ship Plating under Reversed Bending. Ph.D. thesis, MIT, 2000.
[17] Teng X, Wierzbicki T. Multiple impact of beam-to-beam. MIT Impact and Crashworthiness Laboratory, Technical Report 85, June 2002.
[18] Zheng L, Wierzbicki T. Numerical simulation of the impact damage of a box column by a rigid mass. MIT Impact and Crashworthiness Laboratory, Technical Report 83, May 2002.
[19] Parkes EW. The permanent deformation of an encastre beam struck transversely at any point in its span. Proc Inst Civil Eng 1958;10:277–304.
[20] Calder CA, Goldsmith W. Plastic deformation and perforation of thin plates resulting from projectile impact. Int J Solids Struct 1971;7:863–81.
[21] Zhang TG, Yu TX. A note on a 'velocity sensitive' energy-absorbing structure. Int J Impact Eng 1989;8:43–51.
[22] Tam LL, Calladine CR. Inertia and strain-rate effects in a simple plate-structure under impact loading. Int J Impact Eng 1991;11(3):349–77.
[23] Wierzbicki T. Concertina tearing of metal plates. Int J Solids Struct 1995;32(19):2923–43.
[24] Wierzbicki T, Trauth KA, Atkins G. On diverging concertina tearing. J Appl Mech Trans ASME 1998;65:990–7.
[25] Wierzbicki T, Xue L. Aircraft impact damage of steel structures. Proceedings of the 12th International Scientific and Technological Conference on Transport and Building Infrastructure in Crisis Situation, Warsaw-Rynie, Poland, June, 2002.